Nuclear Physics A441 (1985) 420-444

ROTATIONAL CONSEQUENCES OF STABLE OCTUPOLE DEFORMATION IN NUCLEI

W. NAZAREWICZ* and P. OLANDERS

Department of Mathematical Physics, Lund Institute of Technology, S-221 00 Lund, Sweden

Received 22 October 1984
(Revised 25 March 1985)

Abstract: The characteristic features of high-spin spectra of octupole-deformed nuclei are demonstrated by means of Woods-Saxon-Bogolyubov cranking calculations. The rotational spectra of Ra and Th nuclei are studied. The experimental data suggests shape changes with increasing neutron number from $N \simeq 130$ (nearly spherical shapes) through $N \simeq 134$ (octupole-deformed shapes) to $N \simeq 140$ (well-deformed reflection-symmetric shapes). The octupole mixing between the high-j intruder states and normal-parity orbitals leads to specific patterns of quasiparticle spectra characterised by a quantum number referred to as simplex. The influence of octupole deformation on high-spin properties of nuclear spectra like spin alignment, band interaction, etc. are discussed.

1. Introduction

The concept of spontaneous breaking of intrinsic reflection symmetry in nuclei has been supported in recent years both from the experimental and the theoretical side [see e.g. refs. [1-4]) where further references to the earlier literature can be found]. In particular the occurrence of octupole-deformed shapes could explain the appearance of rotational bands characterized by spin states of alternating parity $p = (-1)^I$ connected by enhanced E1 transitions. Such bands have recently been observed [5-11]) in several transitional nuclei around ^{222}Th.

The present work extends the investigations of refs. [3,4]). In a previous study [3]) potential-energy surfaces have been calculated for axially-symmetric and reflection-asymmetric deformations, using the Strutinsky method with a deformed Woods-Saxon potential. An island of octupole-deformed nuclei was found in the light Ra-Th region and the best prospects for ground-state octupole deformation in mass regions below $A \cong 200$ were found around ^{146}Ba. In ref. [4]) some of the high-spin consequences of octupole shape in light actinides were discussed. It was shown that the octupole deformation leads to a more collective pattern of quasiparticle excitations in the rotating nucleus.

The purpose of this work is to study some of the features of the rotational spectra which may be relevant in the analysis of nuclear systems with octupole deformation.

* On leave of absence from Institute of Physics, Technical University, UL. Koszykowa 75, Pl-00662 Warsaw, Poland.

Sect. 2 describes the cranking formalism for reflection-asymmetric shapes by applying the relevant S_1 symmetry. In sect. 3 arguments based on experimental data are given for stable octupole deformations at high spins in several Ra-Th nuclei. Finally, the results of more realistic cranking-shell-model calculations based on an octupole-deformed Woods-Saxon potential are presented in sect. 4.

2. Cranking formalism in the presence of odd-multipole deformations

In the framework of the cranking model the hamiltonian in a rotating frame (routhian) is

$$H^{\omega} = H - \omega J_1 , \tag{1}$$

where H is the intrinsic nuclear hamiltonian usually including a single-particle deformed average field V and a two-body pairing interaction. In refs. [12,13]) the main self-consistent symmetries (SCS) are discussed:

(i) time-reversal T;

(ii) space inversion (parity) P;

(iii) three rotations R_κ through the angle π around the three principal axis of the nuclear field; the finite symmetry group defined by these three rotations is called D_2;

(iv) three reflections through planes containing two principal axes of the nuclear field, $S_\kappa = P \cdot R_\kappa^{-1}$.

The above symmetries were employed by Goodman [12]) to a reflection-symmetric hamiltonian within the cranking model (P is SCS). Bohr and Mottelson [13]) studied general properties of rotational spectra in terms of the particle-rotor model, also including the case of intrinsic parity violation. They pointed out the usefulness of the S_1 operator in the classification of spectra of pear-shaped nuclei. Theoretical calculations of single-particle states in an octupole-deformed potential without inclusion of the pair field have been carried out previously [14,15]) in a study of the mass distribution of heavy-ion-induced fission. Recently [4,16]) the cranking formalism with pairing has been employed to discuss the quasiparticle spectra in reflection-asymmetric nuclei. In this section we briefly discuss the symmetries of the deformed nuclear average field and the rotational consequences thereof. We also give explicit formulas for the "good-simplex" basis and its relation to the "good-signature" basis.

Due to the cranking term $-\omega J_1$ in the hamiltonian (1) the only symmetries which can possibly remain are P, R_1 and S_1 ($[P, J_1] = [R_1, J_1] = [S_1, J_1] = 0$).

To discuss the possible nuclear shapes invariant with respect to the above SCS we expand the nuclear deformed average field in spherical harmonics:

$$V(\boldsymbol{\rho}) = \sum_{L,M} h_{LM}(\rho) Y_{LM}(\Omega) , \tag{2}$$

where, because of the hermicity of V,

$$h_{L-M}(\rho) = (-1)^M h^*_{LM}(\rho) . \tag{3}$$

Spherical tensors Y_{LM} transform as

$$R_1 Y_{LM} R_1^{-1} = (-1)^L Y_{L-M}, \tag{4}$$

$$P Y_{LM} P^{-1} = (-1)^L Y_{LM}, \tag{5}$$

and consequently

$$S_1 Y_{LM} S_1^{-1} = Y_{L-M}. \tag{6}$$

In many cases the field V commutes both with P and R_1. The eigenstates $|\alpha, \pi, r\rangle$ of H^ω can then be characterized by the intrinsic parity π and the signature quantum number r which is the eigenvalue of the R_1 operator. The most general form of the field V which is invariant with respect to P and R_1 is

$$V_{P,R_1}(\boldsymbol{\rho}) = \sum_{\substack{L \\ (L=\text{even})}} u_{L0}(\rho) Y_{L0}(\Omega) + \sum_{\substack{L,M>0 \\ (L=\text{even})}} u_{LM}(\rho) i^M [Y_{LM}(\Omega) + Y_{L-M}(\Omega)], \tag{7}$$

where u_{LM} is a real function of $\rho (h_{LM}(\rho) = i^M u_{LM}(\rho))$. If u_{LM} vanishes for all odd-M values then the field (7) is invariant with respect to the full group D_2.

The signature r is related to the total number of particles A and spin I by the relations [13])

$$R_1^2 = (-1)^A, \tag{8}$$

$$r = \mathrm{e}^{-i\pi I}. \tag{9}$$

Therefore for systems with an even number of nucleons we have

$$r = +1, \qquad I = 0, 2, 4, \ldots, \tag{10}$$

$$r = -1, \qquad I = 1, 3, 5, \ldots, \tag{11}$$

while for systems with odd particle number we have

$$r = -i, \qquad I = \tfrac{1}{2}, \tfrac{5}{2}, \tfrac{9}{2}, \ldots, \tag{12}$$

$$r = +i, \qquad I = \tfrac{3}{2}, \tfrac{7}{2}, \tfrac{11}{2}, \ldots, \tag{13}$$

(with external parity p being equal to $p = +1$ or $p = -1$, independently of I).

In the case of axially-deformed nuclei ($u_{LM} = 0$ for $M \neq 0$) the single-particle states can be characterized by the single-particle angular momentum projection on the symmetry axis, Ω. The good-signature basis can easily be constructed by means of the so-called Goodman transformation [12])

$$|k, \pi, r = -i\rangle = \sqrt{\tfrac{1}{2}}\{-|k, \pi, \Omega_k\rangle + \pi(-1)^{\Omega_k - 1/2}\overline{|k, \pi, \Omega_k\rangle}\}, \tag{14a}$$

$$|k, \pi, r = +i\rangle = \sqrt{\tfrac{1}{2}}\{+\overline{|k, \pi, \Omega_k\rangle} + \pi(-1)^{\Omega_k - 1/2}|k, \pi, \Omega_k\rangle\}, \tag{14b}$$

where $\overline{|k, \pi, \Omega_k\rangle} = T \cdot |k, \pi, \Omega_k\rangle$. (We have adopted the phase convention according to which $T \cdot |\pi jm\rangle = \pi(-1)^{j+m}|\pi j - m\rangle$.) The relation between the states of opposite signature is

$$|k, \pi, r\rangle = U_r|k, \pi, -r\rangle \tag{15}$$

where $U_r = -iR_1T$ is the signature-reversal operator.

Let us now assume that the parity is broken due to some odd-multipole components in (2) but R_1 is SCS. The average field (2) can thus be written in the form

$$V_{R_1}(\boldsymbol{\rho}) = \sum_{\substack{L \\ (L=\text{even})}} u_{L0}(\rho) Y_{L0}(\Omega) + \sum_{L,M>0} u_{LM}(\rho) i^{L+M}[Y_{LM}(\Omega) + (-1)^L Y_{L-M}(\Omega)], \tag{16}$$

where again u_{LM} is a real function of $\rho(h_{LM}(\rho) = i^{M+L}u_{LM}(\rho))$. By comparing (7) and (16) we can see that the only parity-breaking terms in (16) are the non-axial ($M \neq 0$) odd-multipole components like, for instance, the one proportional to $\rho^3 i(Y_{32} - Y_{3-2})$ ($\sim xyz$). For such deformations each band characterized by the good signature r will split into two bands with the same r but opposite parity, forming a so-called parity doublet.

If odd-multipole axial ($M = 0$) deformation components (proportional to Y_{L0}) are present in the nuclear potential neither P nor R_1 are SCS (cf. eqs. (7) and (16)). However, due to relation (6), these odd components are S_1-invariant and just this symmetry can be of particular importance here.

The most general nuclear field V_{S_1} which commutes with S_1 has the form

$$V_{S_1}(\boldsymbol{\rho}) = \sum_L u_{L0}(\rho) Y_{L0}(\Omega) + \sum_{L,M>0} u_{LM}(\rho) i^M [Y_{LM}(\Omega) + Y_{L-M}(\Omega)], \tag{17}$$

where u_{LM} is a real function of $\rho(h_{LM}(\rho) = i^M u_{LM}(\rho))$. V_{S_1} can therefore be both reflection-asymmetric and non-axial. In practice it means that a possible inclusion of non-axial deformations does not change the symmetries of the system.

The eigenvalue s of the S_1 operator is called simplex [4]). When S_1 is SCS the single-particle states can be classified by means of this simplex quantum number.

In ref. [16]) the quantum number σ_t called combined signature was introduced in analogy to the signature exponent quantum number α from ref. [17]). The relation between s and σ_t is similar to the one between r and $\alpha (r = \mathrm{e}^{-i\pi\alpha})$:

$$s = \mathrm{e}^{i\pi\sigma_t}. \tag{18}$$

The square of the S_1 operator is related to the total number of fermions. By means of eq. (8) we have

$$S_1^2 = PR_1^{-1}PR_1^{-1} = R_1^{-2} = (-1)^A. \tag{19}$$

The rotational band with simplex s is characterized by spin states I of alternating parity [13])

$$p = s\,\mathrm{e}^{-i\pi I}. \tag{20}$$

Thus for systems with an even number of nucleons we have

$$s=+1(\sigma_t=0)\,, \qquad I^p=0^+,1^-,2^+,3^-,\dots, \tag{21}$$

$$s=-1(\sigma_t=1)\,, \qquad I^p=0^-,1^+,2^-,3^+,\dots, \tag{22}$$

while for systems with odd particle number we have

$$s=+i(\sigma_t=+\tfrac{1}{2})\,, \qquad I^p=\tfrac{1}{2}^+,\tfrac{3}{2}^-,\tfrac{5}{2}^+,\tfrac{7}{2}^-,\dots, \tag{23}$$

$$s=-i(\sigma_t=-\tfrac{1}{2})\,, \qquad I^p=\tfrac{1}{2}^-,\tfrac{3}{2}^+,\tfrac{5}{2}^-,\tfrac{7}{2}^+,\dots. \tag{24}$$

As for systems with good signature but parity-violating deformations the energy shift between the parity doublets arises here from a tunneling between the left-hand and right-hand orientation of the system. This staggering between the opposite parity states is in lowest order independent of I.

To take advantage of the S_1 symmetry a new basis must be constructed. The Goodman transformation in this case reads

$$|k,s=+i\rangle=\sqrt{\tfrac{1}{2}}(-|k,\Omega_k\rangle+(-1)^{\Omega_k-1/2}\overline{|k,\Omega_k\rangle})\,, \tag{25a}$$

$$|k,s=-i\rangle=\sqrt{\tfrac{1}{2}}(\overline{|k,\Omega_k\rangle}+(-1)^{\Omega_k-1/2}|k,\Omega_k\rangle)\,. \tag{25b}$$

The relation between the states of opposite simplex is

$$|k,s\rangle=U_s|k,-s\rangle\,, \tag{26}$$

where $U_s=-iS_1T$ is the simplex-reversal operator.

It can be convenient to express the basis (25) in the parity-signature representation (14). To do this we separate the positive- and negative-parity component in the wave function $|k\rangle$:

$$|k,\Omega_k\rangle=|k,\pi=+,\Omega_k\rangle+|k,\pi=-,\Omega_k\rangle \tag{27}$$

and combine eqs. (14) and (25). As a result we obtain

$$|k,s=+i\rangle=|k,\pi=+,r=-i\rangle+(-1)^{\Omega_k-1/2}|k,\pi=-,r=+i\rangle\,, \tag{28}$$

$$|k,s=-i\rangle=|k,\pi=+,r=+i\rangle-(-1)^{\Omega_k-1/2}|k,\pi=-,r=-i\rangle\,. \tag{29}$$

In the mirror-symmetric case the simplex quantum number is equal to

$$s=-\pi r \tag{30}$$

and the corresponding relation between σ_t, α and π reads [16])

$$\sigma_t=\begin{cases}\alpha+1, & \text{for } \pi=-\,,\\ \alpha+0, & \text{for } \pi=+\,.\end{cases}$$

It is worth noting that the energetically favoured one-quasiparticle states built on high-j intruder orbitals ($j=N+\frac{1}{2}$) have simplex quantum number $s=+i$ as they have signature $r=i(-1)^{N+1}$ and parity $\pi=(-1)^N$.

The non-zero matrix elements of j_1 are

$$\langle k, s=+i|j_1|k', s=+i\rangle$$

$$=-\langle k, s=-i|j_1|k', s=-i\rangle$$

$$=\begin{cases} \langle k|j_1|k'\rangle = \sum_{\pi} \langle k, \pi, r=-i|j_1|k', \pi, r=-i\rangle\,, & \text{for } \Omega_k \neq \Omega_{k'} \quad (31) \\ -\langle k|j_1|\bar{k}'\rangle = \sum_{\pi} \pi\langle k, \pi, r=-i|j_1|k', \pi, r=-i\rangle\,, & \text{for } \Omega_k = \Omega_{k'} = \frac{1}{2}\,. \quad (32) \end{cases}$$

The general structure of the HFBC equations and their solutions remains the same in the simplex representation as in the parity-signature representation. The simplex of the rotating vacuum is $s=+1$ and the simplex of excited n-quasiparticle configuration is obtained by multiplying with the simplex of each quasiparticle:

$$s_{n\text{q.p.}} = s_1 \times s_2 \times s_3 \times \cdots \times s_n \times 1$$

$$(\sigma_{\text{t},n\text{q.p.}} = \sigma_{\text{t}_1} + \sigma_{\text{t}_2} + \cdots + \sigma_{\text{t}_n} + 0)\,. \tag{33}$$

3. Experimental information on the yrast spectra of Ra-Th nuclei

Until very recently the only information about yrast spectra of nuclei in the $A \simeq 222$ mass region was based on α- and β-decay studies and was therefore limited to low spins. The lack of experimental high-spin data results partly from experimental difficulties associated with this mass region. The very short lifetimes of transitional Ra-Th nuclei together with strong competition from the fission channel and the necessity to use non-standard beams and targets, has strongly limited the possible kind of reactions. In spite of these difficulties recent experiments on ^{218}Ra [refs. [5,8])], ^{222}Th [refs. [6,7])], ^{219,220}Ra [refs. [8,9])] and ^{220,224}Th [ref. [10])], show that it is possible to extend the spectra of $A \simeq 222$ nuclei at least to spins around $17\hbar$, which emphasizes the importance of detailed theoretical calculations of the high-spin spectra of these nuclei. In this section we shall focus our attention on such experimental information on the $N \simeq 134$ Ra and Th isotopes as can support the prediction of octupole deformations in $N \simeq 134$ Ra-Th nuclei.

In octupole-deformed even-even nuclei the positive-parity ground-state band and the low-lying negative-parity rotational band should form a *single* $s=+1$ band (cf. eq. (21)).

Such a structure has recently been observed at high spin in several nuclei from the Ra-Th region. This is illustrated in figs. 1 and 2, which display the energy displacement δE between the positive- and the negative-parity bands in a series of Ra and Th isotopes together with the rotational frequency ratio ω^-/ω^+. The quantity δE is defined as

$$\delta E(I) = E(I^-) - \tfrac{1}{2}(E((I+1)^+) + E((I-1)^+))\,. \tag{34}$$

In the limit of stable octupole deformation $\delta E(I)$ should be close to zero, and at

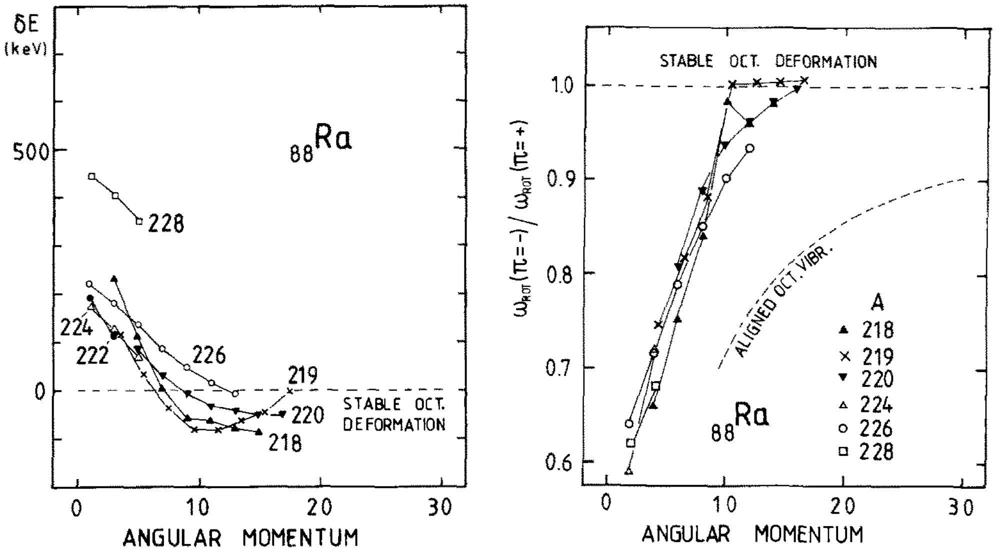

Fig. 1. The displacement of the energy between the positive- and the negative-parity bands (left-hand side), and the ratio of rotational frequencies of the positive- and negative-parity bands (right-hand side) as a function of angular momentum for a series of radium isotopes. The experimental data were taken from refs. [5,8,9,11,18-20]).

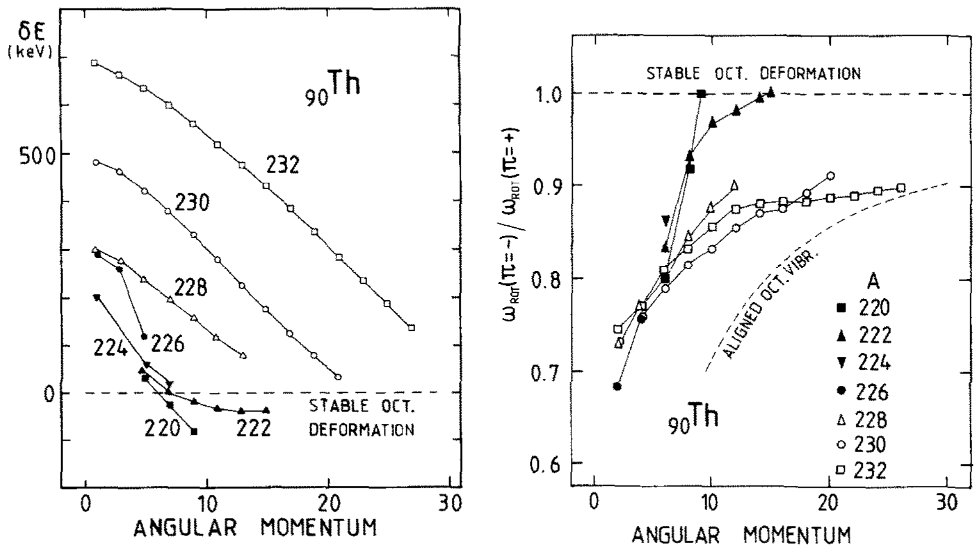

Fig. 2. Similar to fig. 1, but for a series of thorium isotopes. The experimental data were taken from refs. [6,10,18,21-23]).

the same time the ratio between the rotational frequencies of the positive- and the negative-parity bands

$$\frac{\omega^{-}(I)}{\omega^{+}(I)} = 2\frac{E(I+1^{-})-E(I-1^{-})}{E(I+2^{+})-E(I-2^{+})} \tag{35}$$

should approach one. It is clear from figs. 1 and 2 that both quantities given by eqs. (34) and (35) approach at high spins the stable octupole limit for ^{219,220}Ra and ^{220,222}Th nuclei.

For comparison, another limit, the limit of aligned octupole vibration [24]) is shown in figs. 1 and 2. Here

$$\frac{\omega^{-}(I)}{\omega^{+}(I)} = \frac{2I-5}{2I+1}. \tag{36}$$

We assume that the negative-parity band has a pure vibrational character and that the alignment of the octupole phonon is $j_{\mathrm{oct}} = 3\hbar$. It is seen that the negative-parity bands in the heavier Th isotopes, especially in ^{232}Th, can be interpreted in terms of octupole vibrations.

Several different mechanisms can be responsible for the low-spin staggering between the negative- and the positive-parity states of octupole-deformed nuclei. The most important are:

(a) The tunneling through the octupole barrier which leads to the energy splitting of the parity doublet [see e.g. refs. [13,25])].

(b) The Coriolis couplings to $K \neq 0$ octupole bands which increase the moment of inertia of the lowest $K=0$ negative-parity band [see e.g. refs. [24,26-28])].

(c) The interaction between the positive-parity deformed band and the positive-parity band existing in a local spherical minimum [4]).

(d) The quadrupole-octupole coupling [29]); especially important for the quadrupole- and octupole-soft nuclei, like $^{218-220}$Ra or ^{220}Th.

Another signature of octupole instability in the Ra-Th nuclei comes from the electromagnetic transition probabilities. Experimental data show a strong competition between the stretched intraband E2 transitions and the very enhanced stretched E1 transitions connecting the opposite-parity states. The experimentally determined E1 transition rates in ^{225}Ac [ref. [30])] and ^{218}Ra [ref. [8])] are of the order of 10^{-2} W.u. which is about two orders of magnitude larger than the typical B(E1) values in the deformed heavier nuclei in the actinide region and three to four orders of magnitude larger than for typical single-particle B(E1) rates.

This "collective" dipole radiation originates in the shift between the centre of charge and the centre of mass, around which the nucleus rotates. This polarisation effect due to octupole deformation have been discussed by Bohr and Mottelson [31]) and Strutinsky [32]) within the liquid drop model. The value of the induced dipole moment was estimated to be proportional to the quadupole and octupole deformations β_2 and β_3:

$$D = cAZe\beta_2\beta_3 \,, \tag{37}$$

where both the magnitude of the constant c and its sign turned out to be very sensitive to the model assumptions (the Bohr and Mottelson value is -5.2×10^{-4} fm, while the one obtained by Strutinsky is $+6.9\times10^{-4}$ fm).

At present, there are not many direct experimental data for the transition rates in the discussed region of nuclei. However, some valuable information about the E1 enhancement can be deduced from the $B(\mathrm{E1})/B(\mathrm{E2})$ branching ratios [6,8,9]). For the lighter Ra isotopes and for ^{222}Th the ratios scatter around an average of $2\times10^{-6}\ \mathrm{fm}^{-2}$ which corresponds to a dipole moment of the order of 0.45 $e\cdot$fm. The octupole deformations that were deduced by using eq. (37) are, however, two to three times larger than those predicted by Strutinsky-type calculations [1-3]).

By means of eq. (37) we can calculate the $B(\mathrm{E1})/B(\mathrm{E2})$ branching ratio:

$$\frac{B(\mathrm{E1})}{B(\mathrm{E2})} \simeq 2.694c^2A^{2/3}\langle\beta_3^2\rangle\ \mathrm{fm}^{-4} \,. \tag{38}$$

Formula (38) obviously accounts for the dispersion of the β_3 fluctuations. It is clear, that for very shallow octupole potentials the value of $\langle\beta_3^2\rangle$ will be considerably large (i.e. $\langle\beta_3^2\rangle \gg \beta_{3\mathrm{eq}}^2$). Therefore the large values of the $B(\mathrm{E1})/B(\mathrm{E2})$ branching ratio for transitional nuclei like $^{218-220}$Ra and ^{222}Th can be due to *both* the possible presence of octupole deformation at high spin and to strong anharmonic effects which increase the β_3 dispersion. Another effect which can influence the $B(\mathrm{E1})$ and $B(\mathrm{E3})$ values is the Coriolis coupling to the $K\neq0$ octupole states. It is well known [26,27]) that it accounts for about 40% of the $B(\mathrm{E3})$ strength in well-deformed actinides. In the transitional Ra-Th nuclei the effect of the Coriolis coupling on the transition rates is not so strong because of a dramatic lowering of the $K=0$ states and it can even lead to a *reduction* of the $B(\mathrm{E3})$ values [28]).

The simple estimates of β_3 based on the $B(\mathrm{E1})/B(\mathrm{E2})$ branching-ratio values [see e.g. ref. [6])] cannot then be very conclusive. The pronounced reduction of the branching ratio in ^{226}Ra compared to ^{222}Th can only partly be explained by the difference in their octupole equilibrium deformations (0.083 and 0.096, respectively) calculated in ref. [3]).

To get an idea about possible spin alignments or deformation changes, which may occur along the yrast lines of positive and negative parity, it is instructive to plot the kinematical ($J^{(1)}\equiv I_1/\omega$) and the dynamical ($J^{(2)}\equiv \mathrm{d}I_1/\mathrm{d}\omega$) moments of inertia versus rotational frequency. Fig. 3 shows a summary of the experimental moments of inertia of the even-even radium and thorium isotopes with neutron numbers $130\leq N\leq142$. The energy surfaces in the (β_2, β_3) plane calculated with a Woods-Saxon potential are given in fig. 4 for the even-even Th nuclei [the corresponding plots for Ra are given in ref. [3])]. Our calculations predict a transition

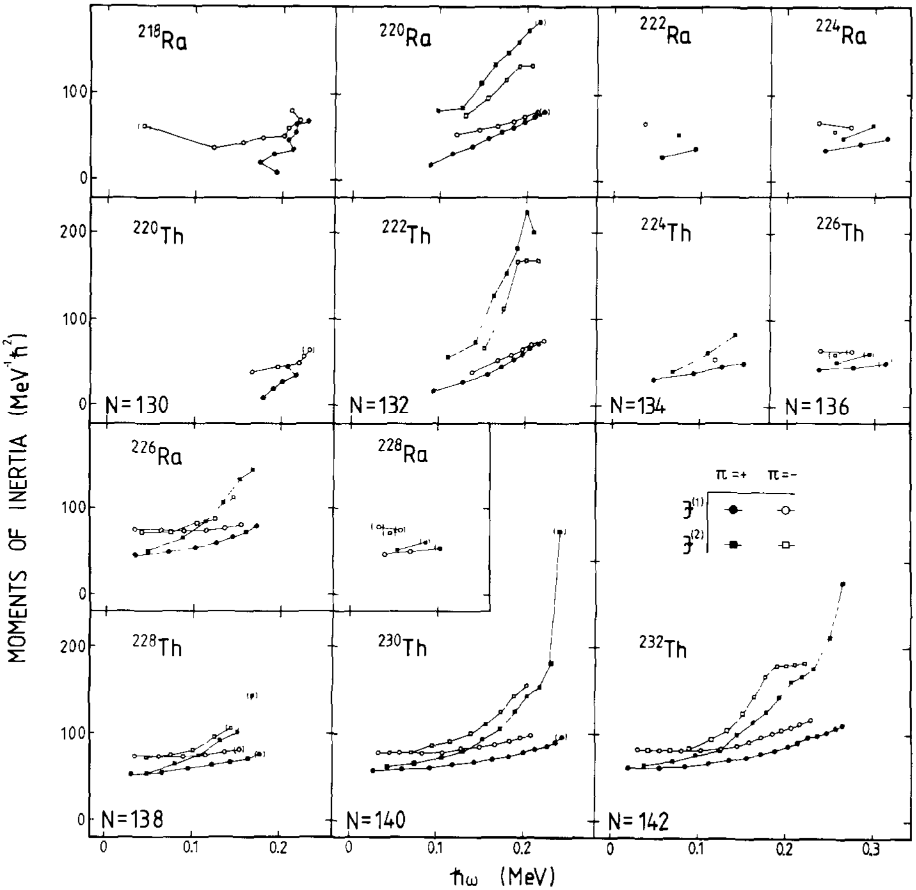

Fig. 3. Experimental moments of inertia, $J^{(1)}$ and $J^{(2)}$ of positive- and negative-parity bands in the even-even Ra-Th isotopes with $130 \leq N \leq 142$.

from spherical shape to quadrupole well-deformed shapes with increasing neutron number.

For $N = 130$ the ground states are predicted to be spherical (see fig. 4). The experimental data for ^{218}Ra and ^{220}Th show that at low spins these nuclei behave like soft vibrators. It has been suggested [3,4]) that collective rotational excitations enhance and stabilize quadrupole as well as octupole deformations in very soft nuclei like ^{218,220}Ra and ^{220}Th. One should therefore expect that with increasing angular momentum these nuclei will move into the (β_2, β_3) deformation plane along the trajectory indicated in fig. 4 for ^{220}Th. The $J^{(1)}$ moments of inertia ($J^{(2)}$ is not plotted here) in ^{218}Ra and ^{220}Th show irregularities (backbendings) around frequency $\hbar\omega = 0.21$ MeV.

For $N = 132$ the calculations yield a stable octupole deformation in ^{222}Th while ^{220}Ra is predicted [3]) to be spherical in its ground state, but very soft along the

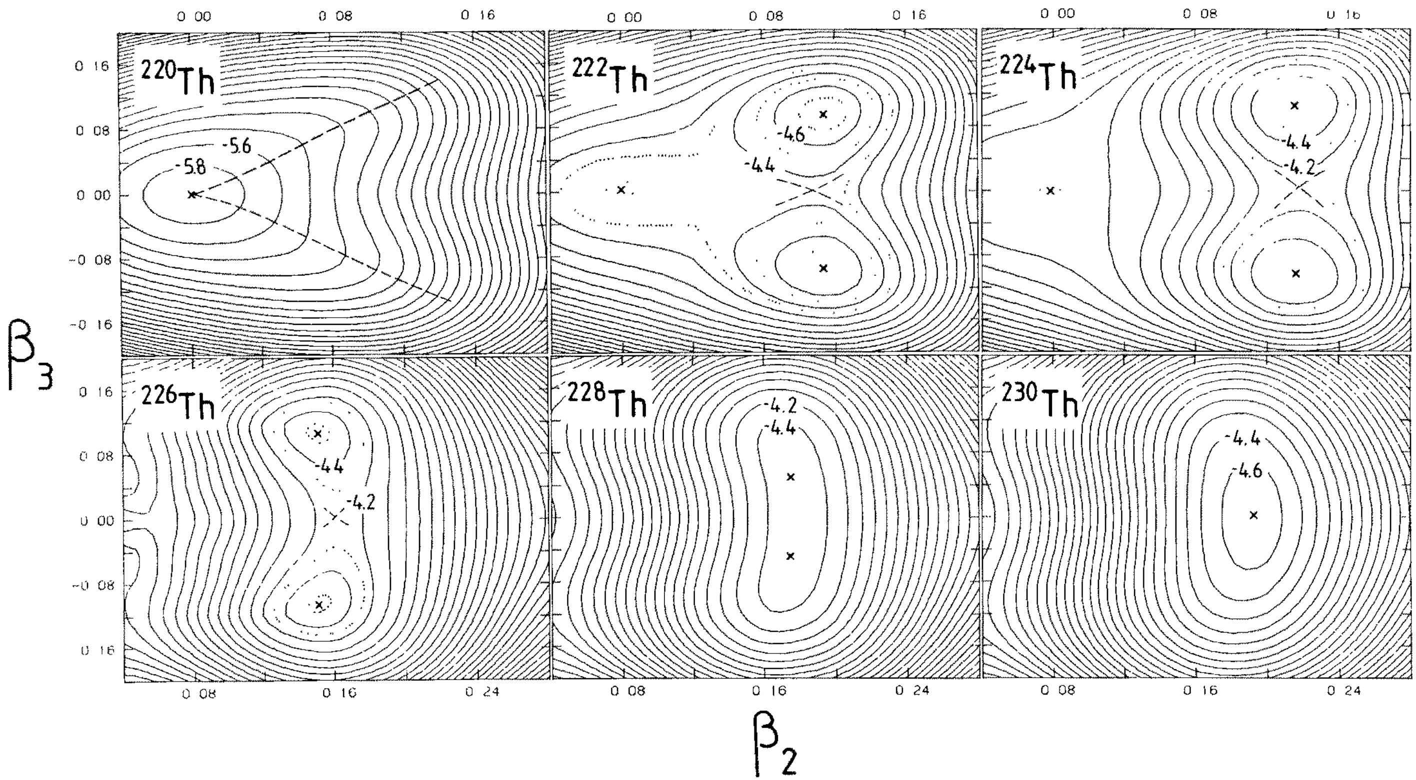

Fig. 4. The Strutinsky energy for $^{220-230}$Th obtained from the Woods-Saxon potential as a function of β_2 and β_3 [for more details of the calculations, see ref. [3])]. Note that the combined (β_2, β_3) softness of ^{220}Th (indicated by a dashed line) evolves into the minima with $\beta_2 \neq 0$ and $\beta_3 \neq 0$ in ^{222}Th. The energy separation between the (solid) contour lines is 200 keV. The dotted contour lines mark the additional 100 keV separations. Notice the different scale in β_2 for $^{220-224}$Th and $^{226-230}$Th.

(β_2, β_3) trajectory similar to the one for ^{220}Th indicated by the dashed line in fig. 4. In ^{222}Th the single $s = 1$ rotational band is formed at frequency $\hbar\omega \simeq 0.15$ MeV. In the second moment of inertia $J^{(2)}$ there is a clear smooth upbending centered around $\hbar\omega = 0.20$ MeV. We interpret it in sect. 5 as a reflection of a neutron band crossing. In ^{220}Ra the single $s = 1$ band is formed at a slightly higher rotational frequency, and at low spin this nucleus approaches the vibrational limit [9]). As for ^{222}Th a smooth upbending in the negative-parity band is observed at $\hbar\omega \simeq 0.20$ MeV. The potential energy surface for ^{222}Th shows a secondary equilibrium configuration at spherical shape which is close in energy to the deformed ground state. It can interact with the deformed 0^+ level and lower its energy [4]) leading to an additional contribution to the energy splitting between the negative- and positive-parity bands at low spins.

For $N = 134$ and $N = 136$ well-deformed equilibrium shapes are expected. The total energy surfaces have a minimum valley in the β_3 direction at a fairly constant β_2 (see fig. 4). Unfortunately, the experimental data for $^{222-224}$Ra and $^{224-226}$Th are rather poor, and therefore not very conclusive for the hypothesis of stable octupole deformation. The increase of the moments of inertia for these nuclei compared to the $N = 132$ isotones reflects their larger equilibrium deformations.

For $N = 138$ the calculations predict very flat octupole minima, with a barrier smaller than 100 keV. The negative-parity bands in ^{226}Ra and ^{228}Th were reproduced by simplified Coriolis-coupling calculations [21,33]) [see however also ref. [28])]. The ^{226}Ra nucleus has, however, considerably larger octupole deformation $(\beta_3 = 0.08)$ compared to the one in ^{228}Th $(\beta_3 = 0.05)$, which can explain why it is closer to the stable octupole limit of figs. 1 and 2. In fact, for $\hbar\omega \simeq 0.17$ MeV the moments of inertia of the negative- and positive-parity bands in ^{226}Ra start to approach each other. The pronounced enhancement of the $B(\mathrm{E1})/B(\mathrm{E2})$ branching ratio with increasing spin observed [11]) in ^{226}Ra suggest the octupole deformation in this nucleus at high rotational frequency.

For $N > 138$ no stable octupole deformed shapes are theoretically predicted. The negative-parity bands in $^{230-232}$Th can be interpreted [27,34]) in terms of octupole vibrations. The second moments of inertia $J^{(2)}$ show a smooth upbending around $\hbar\omega = 0.20$ MeV (both for ^{230}Th and ^{232}Th) and very strong alignment at $\hbar\omega \simeq 0.24$ MeV in ^{230}Th and at $\hbar\omega \simeq 0.26$ MeV in ^{232}Th. Calculations [35-37]) explain this double-humped structure of $J^{(2)}$ as due to the $j_{15/2}$ neutron and $i_{13/2}$ proton crossings.

The only odd-mass nucleus presented here, ^{219}Ra (fig. 5), $N = 131$, exhibits less regular rotational pattern than its $N = 132$ even-even neighbours. The second moment of inertia increases rapidly at $\hbar\omega \simeq 0.2$ MeV, which can be due to spin alignment and/or possible deformation changes (see subsect. 4.2). The preliminary data of ref. [8]) show two smooth positive- and negative-parity rotational sequences forming a clear parity doublet (cf. fig. 2) which, together with the enhanced E1 transition rates for this nucleus, suggests an interpretation of the high-spin spectrum of ^{219}Ra in terms of stable octupole deformation.

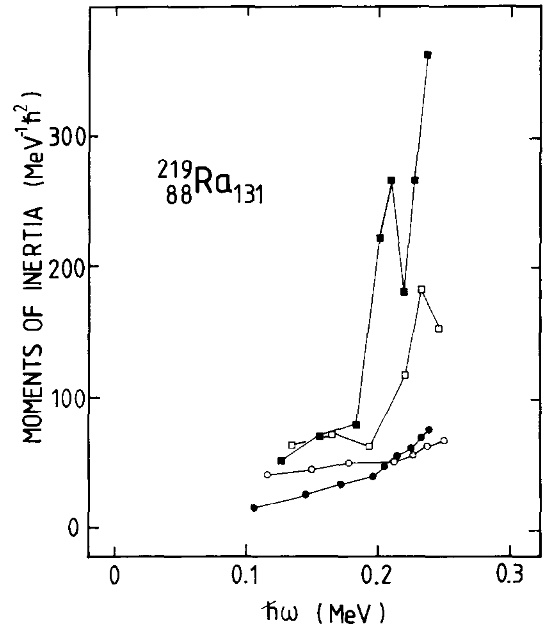

Fig. 5. Similar to fig. 3, but for ^{219}Ra. The experimental data were taken from ref. [8]). The parity and spin assignments are uncertain for all the states (not indicated by parentheses in this plot).

4. Woods–Saxon cranking calculations

In order to draw some quantitative conclusions on the high-spin behaviour of nuclei around ^{224}Th cranking-type calculations were carried out. In the present study we use the same model as in refs. [3,4]) where detailed information about the potential, parameters, etc. are given.

We restrict ourselves to axially symmetric shapes which is phenomenologically justified in the Ra-Th region, where it is a $K^{\pi}=0^{-}$ octupole band that is observed at low energies and, in addition, there is no evidence for low-lying γ-vibrational bands. At very high angular momenta, however, the non-axial degrees of freedom can be of some importance because of the γ-polarisation of nuclear shape induced by aligned quasiparticles. The ground state shapes of Ra-Th nuclei can be fairly well described in terms of three deformation parameters: β_2, β_3 and β_4. In case of nonaxial distortion the most general simplex-conserving average field is given by eq. (17). After assuming that the intrinsic system is defined by the quadrupole deformation ($u_{21}=u_{2-1}=0$ in (17)) and, furthermore, that the hexadecapole field has the same main axis as the quadrupole field, the minimal number of independent deformation parameters is nine ($\lambda=2$, $\mu=0$, 2; $\lambda=3$, $\mu=0$, 1, 2, 3; $\lambda=4$, $\mu=0$, 2, 4). Further investigations in this direction have been planned.

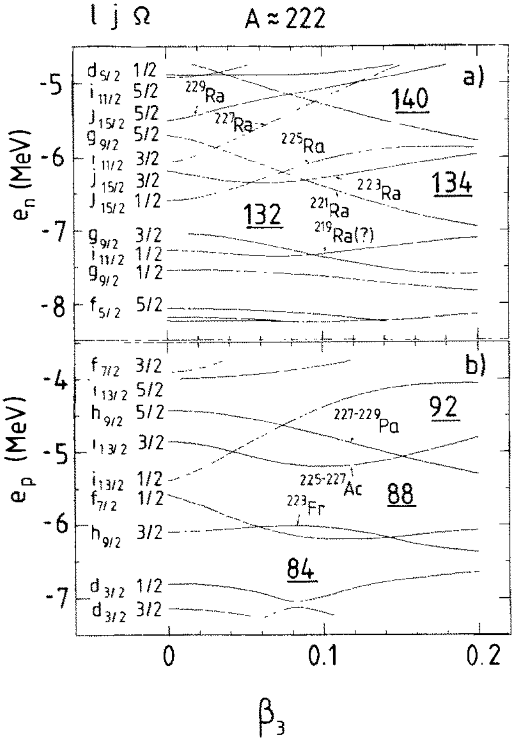

Fig. 6. The Woods-Saxon single-particle neutron (a) and proton (b) orbitals plotted versus octupole deformation β_3. The other deformation parameters $\beta_2 = 0.15$ and $\beta_4 = 0.08$ correspond approximately to the calculated [3]) equilibrium deformations for the transitional Ra-Th nuclei. The arrows indicate the theoretical spin assignments. The states are labelled by the Ω quantum number and by the spherical labels (l, j) which are approximately valid at $\beta_3 = 0$. The experimental ground-state spin for the even-odd $^{221-229}$Ra isotopes were taken from ref. [38]) and the corresponding ones for odd-proton nuclei from refs. [30,39]). The ground state of ^{219}Ra can, most probably, be assigned to the "$i_{11/2}$" ($\Omega = \frac{1}{2}$) orbital with decoupling factor $a \approx -2.5$ which will therefore lead to the $I^\pi = \frac{3}{2}^+$ ground state in this nucleus.

The realiability of the presented results depends to a large extent on a correct theoretical description of the single-particle orbitals. Fig. 6 illustrates the Woods-Saxon single-particle levels plotted versus octupole deformation β_3. The other deformation coordinates are defined by $\beta_2 = 0.15$ and $\beta = 0.08$ corresponding approximately to the equilibria for most of the octupole-deformed Ra-Th nuclei.

The ground state spins in a series of Ra isotopes has recently been determined [38]) to be $\frac{5}{2}$ (^{221}Ra), $\frac{3}{2}$ (^{223}Ra), $\frac{1}{2}$ (^{225}Ra), $\frac{3}{2}$ (^{227}Ra) and $\frac{5}{2}$ (^{229}Ra). The proposed Woods-Saxon assignments are indicated by arrows in fig. 6a as well as the spin assignments for several odd-proton nuclei (fig. 6b). The correspondence between theoretical level order and ground-state spin values is very good. For a more detailed discussion of single-particle properties in the discussed mass region we refer the reader to refs. [2,30,40-43]).

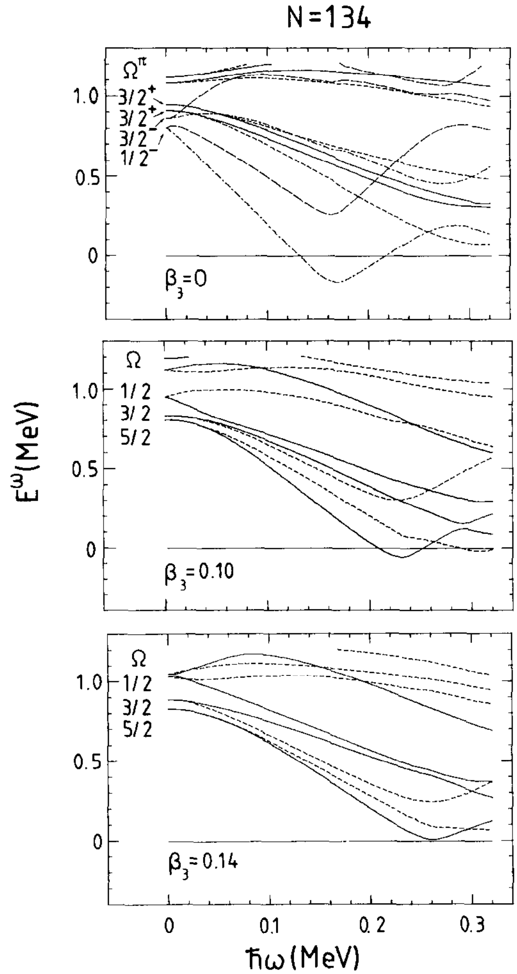

Fig. 7. Neutron quasiparticle routhians for $N = 134$ for $\beta_3 = 0$, 0.1 and 0.14. The quadrupole and hexadecapole deformation parameters $\beta_2 = 0.14$ and $\beta_4 = 0.08$ correspond to the equilibrium deformation of ^{224}Th. The pairing energy gap was kept constant at $\Delta = 0.8$ MeV. Solid lines represent states with simplex $s = +i$ (or $\pi = +1$, $r = -i$ in the $\beta_3 = 0$ diagram) while the short-dashed lines $s = -i$ (or $\pi = +1$, $r = +i$ in the $\beta_3 = 0$ diagram). The dash-dotted and long-dashed lines in the $\beta_3 = 0$ diagram represent states with $\pi = -1$, $r = +i$ and $\pi = -1$, $r = -i$, respectively.

The strong octupole couplings between the $\nu j_{15/2} - \nu g_{9/2}$ and $\pi i_{13/2} - \pi f_{7/2}$ subshells induce the significant $N = 132$, 134, 138, 140 and $Z = 84$, 88, 92 openings in the single-particle spectra. The stable octupole deformations in the transitional actinides can be related to these gaps. In the case of reflection-symmetric shape ($\beta_3 = 0$) the Fermi energies of $Z = 88$, 90 and $N \simeq 134$ nuclei are in the vicinity of very strong aligning high-j, low-Ω orbitals ($j_{15/2}$ ($\Omega = \frac{1}{2}$) and $j_{15/2}$ ($\Omega = \frac{3}{2}$) neutron and $i_{13/2}$ ($\Omega = \frac{1}{2}$) and $i_{13/2}$ ($\Omega = \frac{3}{2}$) proton levels). Calculations without inclusion of

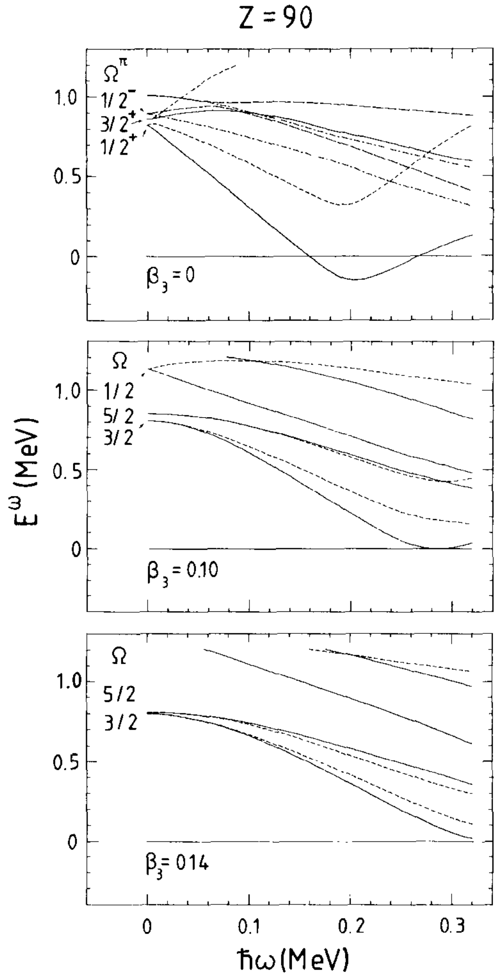

Fig. 8. Similar to fig. 7, but for protons ($Z = 90$).

octupole deformation [44,45]) have therefore predicted sharp band-crossings at a rotational frequency $\omega \simeq 0.18$ MeV/$\hbar$.

The experimental data for ^{220}Ra and ^{222}Th presented in fig. 3 do not show any backbending up to $\hbar\omega \simeq 0.22$ MeV. The smooth, collective behaviour of $J^{(1)}$ versus ω curve for the yrast line in these nuclei was then quite astonishing. In recent papers [4,16]) an explanation of this unexpected result has been given in terms of stable octupole deformation.

It has been demonstrated in refs. [4,16,46]) that the octupole deformation yields an averaging of the quasiparticle alignment. This effect is clearly seen in figs. 7 and 8 which show ^{224}Th quasiparticle routhians E^ω versus rotational frequency, at three values of octupole deformation: $\beta_3 = 0$ (mirror symmetric case), $\beta_3 = 0.10$ [octupole equilibrium deformation of ref. [3])], and $\beta_3 = 0.14$ [which roughly corresponds to results of calculation with the folded-Yukawa potential [1])]. The excitation spectra in the reflection symmetric and asymmetric cases are very different. At $\beta_3 = 0$ the strongly aligned intruder orbitals ($\nu j_{15/2}$ and $\pi i_{13/2}$) slope down very rapidly with increasing ω, leading to a band-crossing with small yrast-yrare interaction at $\hbar\omega \simeq 0.18$ MeV. For $\beta_3 \neq 0$ the pattern becomes more collective: many orbitals have an almost equally large alignment. This "equalisation" effect is illustrated in a better way in figs. 9 and 10 where the contributions to the total spin $\langle L|j_1|L\rangle$ originating from four lowest quasiparticle routhians (two of each simplex) together with their parity contents $\langle L|\pi|L\rangle$ are plotted versus octupole deformation for fixed value of rotational frequency, $\omega = 0.14$ MeV/$\hbar$. Both for protons and for neutrons the alignment of the orbitals originating from high-j intruder states (at $\beta_3 = 0$) is considerably reduced with β_3 and the average parities of the lowest excitations approach zero. At large octupole deformations the mean quasiparticle alignment is about $3.25\hbar$ (neutrons) and $2.25\hbar$ (protons). As discussed in ref. [46]) there are two reasons for this: (a) the strength of the orbitals of the intruders are fragmented by the octupole interaction between several orbitals in which the normal-parity components contribute a smaller and sometimes negative alignment, and (b) the octupole deformation changes the structure of single-particle levels in the vicinity of the Fermi level leading to a relative decrease of components of the low-Ω intruder states in the quasiparticle wave function.

The fragmentation mentioned above leads to a significant decrease of the energy difference between the lowest quasiparticle routhians of opposite simplex (simplex splitting). This effect can be directly related to changes of the $\langle \alpha, \Omega = \frac{1}{2}|j_1|\alpha', \Omega = \frac{1}{2}\rangle$ matrix elements with octupole deformation. The diagonal ones corresponding to decoupling factors of the high-j shell are reduced by about 30% in realistic calculations where the normal-parity $j = (N-1) - \frac{1}{2}$ orbitals are involved [2,40-42]).

With increasing β_3 value the crossing frequency becomes larger. The typical values of $\hbar\omega_c$ at $\beta_3 = 0.1$ are 0.21 MeV and 0.28 MeV for neutrons and protons, respectively.

The band interaction as a function of the Fermi energy, λ, is plotted in figs. 11 (neutrons) and 12 (protons). In the case of $\beta_3 = 0$ (top) both the proton and neutron interaction is very small for almost all nuclei from the Ra-Th region. For $\beta_3 = 0.1$ (bottom) $|V|$ increases considerably for almost all values of N and Z. Comparing fig. 11 with fig. 3 we observe a correlation between the $|V|$ versus λ_n behaviour and the experimental alignment plots. The neutron number $N = 132$ corresponds to a large band interaction and therefore the bumps in the $J^{(2)}$ moments of inertia observed in ^{220}Ra and ^{222}Th nuclei for $\hbar\omega \simeq 0.20$ MeV can be interpreted as caused by a neutron alignment. For $N = 130$ isotones the interaction is small and this may be the reason for the backbending observed in ^{220}Th at $\hbar\omega \simeq 0.20$ MeV. For the $N = 134$ nuclei our calculations predict an alignment at $\hbar\omega_c \simeq 0.20$ MeV but for the moment there are no experimental data available at such high spins to check this result.

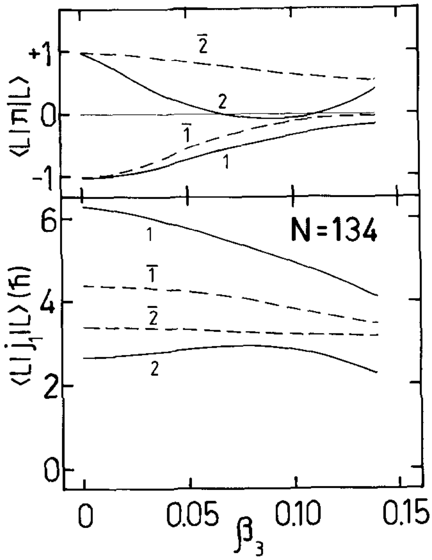

Fig. 9. Quasiparticle parity content $\langle L|\pi|L\rangle$ (top) and quasiparticle alignment $\langle L|j_1|L\rangle$ (bottom) for the lowest neutron quasiparticle states in ^{224}Th. The rotational frequency was kept constant at $\hbar\omega = 0.14$ MeV. The other parameters are the same as in fig. 7.

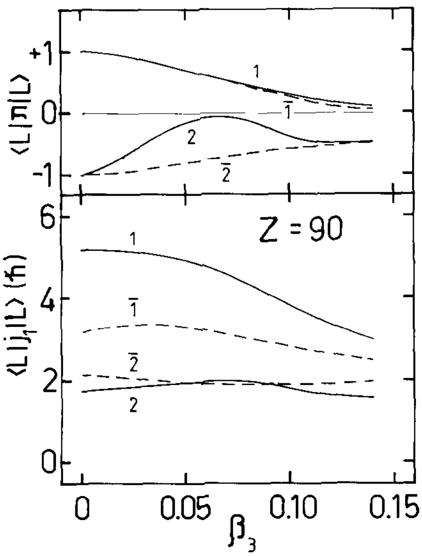

Fig. 10. Similar to fig. 9, but for the lowest proton quasiparticle states in ^{224}Th.

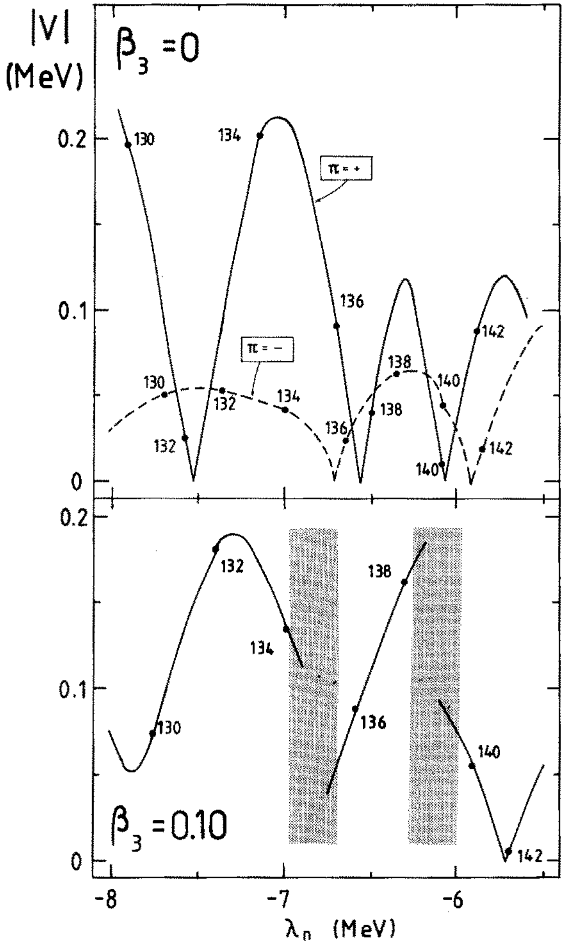

Fig. 11. The neutron band interaction $|V|$ versus Fermi energy λ for $\beta_2 = 0.14$, $\beta_4 = 0.08$ and two values of octupole deformation: $\beta_3 = 0$ (top) and $\beta_3 = 0.10$ (bottom). The particle numbers are indicated by dots. The regions of complex crossings (more than two-quasiparticle levels interact in the same region of $\hbar\omega$) are shaded.

To comment the possible deformation changes with increasing angular momentum we write the total routhian of an n-quasiparticle configuration as

$$E^{\omega}(\beta_3) = E^{\omega}_{g}(\beta_3) + \sum_{L=1}^{n} E^{\omega}_{L}(\beta_3) , \tag{39}$$

where E^{ω}_{g} is the vacuum reference and E^{ω}_{L} are the quasiparticle routhians. For a given value of the rotational frequency the total routhian (39) should be minimized with respect to β_3 to determine the equilibrium deformation.

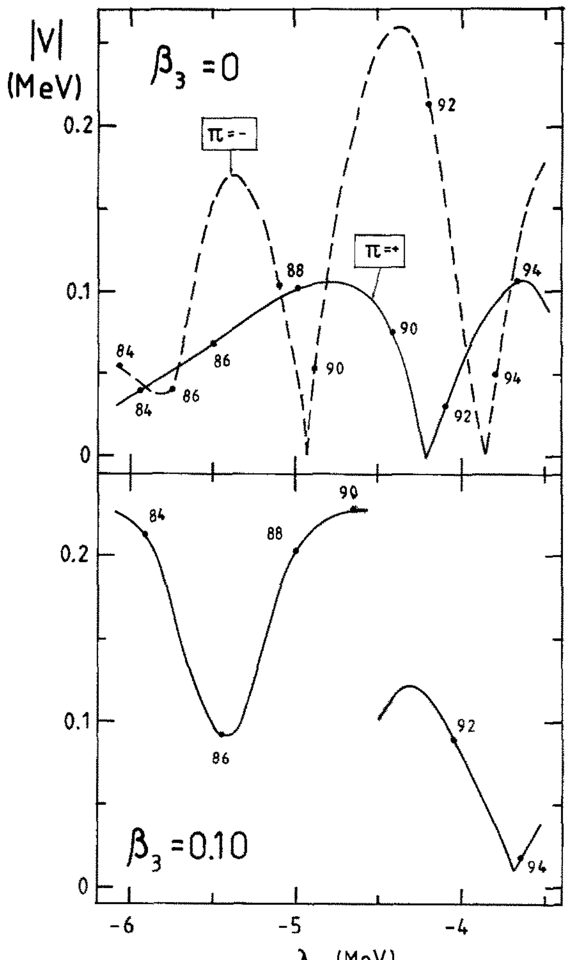

Fig. 12. Similar to fig. 11, but for protons.

This simple prescription for estimating the possible deformation changes with rotational frequency was originally proposed in ref. [47]) and has been applied to study the interplay between the single-particle and shape degrees of freedom in γ-soft nuclei [47,48]). In fig. 13a the sum of the two lowest quasiparticle routhians (for neutrons, $N=134$ and protons, $Z=90$) is plotted as a function of β_3 for a fixed value of rotational frequency ($\hbar\omega=0.14$ MeV). It is seen that this sum (corresponding to a two-quasiparticle excitation) has a pronounced minimum at $\beta_3=0$ indicating a strong β_3-driving tendency towards the mirror-symmetric shape. Apart from the β_3-driving forces of the excited quasiparticles an additional force comes from the core. The reference routhian E_g^ω presented in fig. 13b has minimum at $\beta_3 \simeq 0.11$.

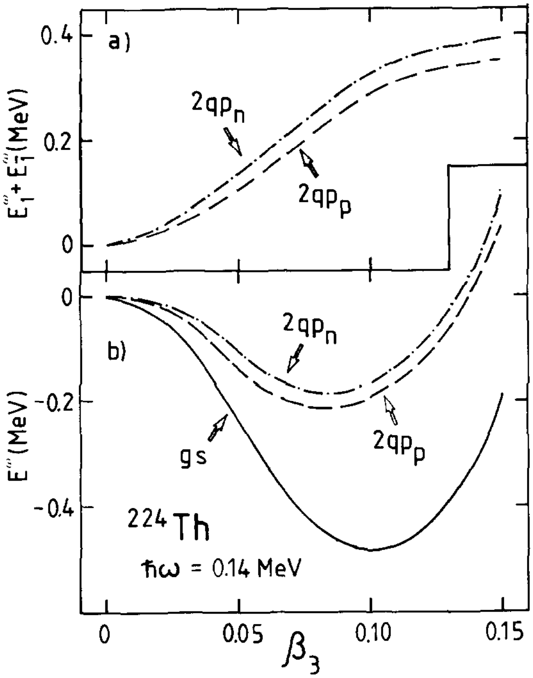

Fig. 13. (a) Sum of the two lowest neutron and proton quasiparticle routhians for ^{224}Th as a function of β_3 at $\hbar\omega = 0.14$ MeV. The other deformation parameters are $\beta_2 = 0.14$ and $\beta_4 = 0.08$. (b) The total routhians for the ground-state, and two-quasiparticle neutron and proton configurations in ^{224}Th.

E^{ω}_{g} was computed according to the formula

$$E^{\omega}_{g}(\beta_3) = V_{Str}(\beta_3) + \langle H^{\omega}\rangle - \langle H^{\omega}\rangle|_{\omega=0} \tag{40}$$

in which the Strutinsky potential V_{Str} of ref. [3]) has been used. Combining these opposite β_3-driving trends we obtain a reflection-asymmetric shape corresponding to $\beta_3 \simeq 0.09$ results for two-quasiparticle neutron or proton bands in ^{224}Th. [A similar conclusion was drawn in ref. [16]) where, however, the discussion is based on the quasiparticle diagrams plotted at quadrupole deformation $\varepsilon = 0.20$ which is not representative for the transitional isotopes of Ra-Th considered here.] It seems, however, that for three or four quasiparticle bands the β_3-driving force will be strong enough to restore the reflection symmetry.

The ground state band of ^{219}Ra presented in fig. 5 shows strong alignments around $\hbar\omega = 0.21$ MeV. The explanation in terms of neutron alignment seems to be questionable as the first band-crossing is supposed to be blocked by the odd quasiparticle.

A possible mechanism for this seemingly unexpected behavior is shown in fig. 14 where the quasiparticle routhians for $N = 131$ are shown versus rotational frequency. At low rotational frequencies the ground-state rotational band corresponds to the filling of the lowest $s = -i$ routhian (labelled by $\bar{1}$ in fig. 14) originating from the

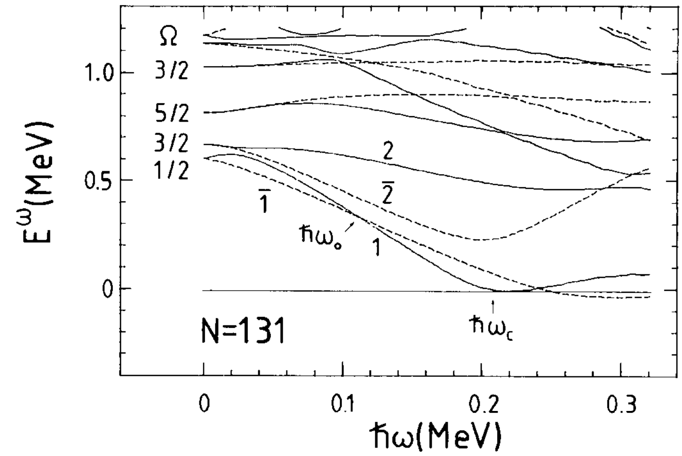

Fig. 14. Neutron quasiparticle routhians for $N = 131$ versus rotational frequency. The deformation parameters used are: $\beta_2 = 0.125$, $\beta_3 = 0.1$, $\beta_4 = 0.07$. The pairing gap, $\Delta = 0.6$ MeV, is slightly decreased compared to the pairing gap used in fig. 7 for ^{224}Th on account of the reduction of the pair field due to the blocking effect.

$i_{11/2}$ ($\Omega = \frac{1}{2}$) orbital (see fig. 6a). However, this quasiparticle level is crossed around $\hbar\omega_0 = 0.11$ MeV by the $s = +i$ routhian carrying larger alignment, which then becomes lower in energy, *simplex inversion*. The $s = -i$ orbital passes smoothly through the area of the first neutron crossing which occurs around $\hbar\omega_c = 0.21$ MeV. Therefore, the smooth unbending due to the band-crossing with the two-quasiparticle band $(1, \bar{2})$ should be observed in the ground-state band of ^{219}Ra. As the states 1 and $\bar{1}$ have very different intrinsic structures (and different values of the simplex quastum number) a strong retardation of the electromagnetic transitions between the corresponding one-quasiparticle bands should be expected. After the first crossing a three-quasiparticle configuration $(1, \bar{1}, 2)$ becomes lowest in energy and, according to the discussion above, also a shape change towards $\beta_3 = 0$ is possible.

6. Conclusions

Experimental evidence as well as theoretical calculations suggest that high-spin spectra in nuclei around ^{224}Th may be interpreted in terms of stable octupole deformation. The main conclusions and results can be summarized as follows:

(i) The quasiparticle spectra of pear-shaped nuclei can be characterized by the simplex quantum number s introduced in ref. [4]) which has similar properties as the signature quantum number in absence of reflection asymmetry. The possible inclusion of non-axial degrees of freedom does not destroy this quantum number. Therefore the cranking-shell-model picture of ref. [17]) remains practically unchanged in the presence of odd-multipole deformations.

(ii) The presence of enhanced E1 transitions in the Ra-Th nuclei can be interpreted as an indication of either stable octupole deformation *or* octupole softness. In particular, it may be difficult, if not impossible, to estimate the β_3 value from experimental $B(\mathrm{E1})/B(\mathrm{E2})$ branching ratios using the liquid-drop formula (37) for the induced dipole moment.

(iii) Stable octupole deformation leads to specific features of quasiparticle spectra:

(a) The quasiparticle alignment of the lowest routhians decreases with β_3 due to the octupole coupling between intruder orbitals and normal-parity states. On the other hand, the average alignment of normal-parity states increases. As a consequence, many quasiparticle routhians have a similar alignment and one-quasiparticle rotational bands with practically indistinguishable high-spin properties are expected in neighbouring odd-mass nuclei [see also the discussion in refs. [4,16])].

(b) The band-crossing frequency increases ($\hbar\omega_c \simeq 0.21$ MeV and 0.28 MeV for neutrons and protons, respectively) compared to the mirror-symmetric case ($\hbar\omega_c \simeq$ 0.18 MeV for both neutrons and protons).

(c) The band interaction generally increases with β_3, the number of zeros is reduced and the regular oscillatory structure of $|V|$ versus λ can no longer be seen. Because of larger number of qusiparticle orbitals which can interact many-level crossings or two-level crossings with practically inactive spectators (cf. fig. 14) often occurs.

(d) The simplex splitting of the lowest routhians is reduced.

(e) The average parity of the lowest aligned quasiparticle excitations is usually close to zero.

(iv) The octupole deformation explains the weak alignment in light actinides. The large value of the proton crossing frequency together with the large band interaction for $Z = 88, 90$ (fig. 12) exclude in practice the chance for strong proton crossing at spins possible to reach experimentally. The neutron band-crossing occurs at lower frequency and it causes a gradual alignment observed experimentally in ^{222}Th and ^{220}Ra (large band interaction for for $N = 132$) and the backbending observed in the yrast line of ^{220}Th (small band interaction for $N = 130$).

(v) The very β_2- and β_3-soft transitional nuclei like ^{220}Th or ^{220}Ra (see fig. 4) will likely become both quadrupole *and* octupole deformed at high spins (cf. also figs. 1 and 2).

(vi) One- or two-quasiparticle excitations are not expected to cause any dramatic change in the octupole deformation. However, the β_3-driving force of a three- or four-quasiparticle excitations is supposedly strong enough to restore the reflection symmetry of the nucleus.

(vii) The experimentally observed unbending in the ground-state band of ^{219}Ra can be explained as caused by the neutron alignment. The band-crossing at $\hbar\omega =$ 0.21 MeV is not blocked by the odd neutron which occupies the $\mathrm{i}_{11/2}$ orbital with an intrinsic structure differing from the orbital involved in the crossing.

Finally, we would like to mention that an alternative explanation of unusual spectra of $N=134$ Ra-Th nuclei has been given in terms of a phenomenological α-cluster model [49,50]). For the moment, however, its relation to the microscopic approach involving stable octupole deformation is not very clear. The low-lying negative-parity states may also be explained in terms of anharmonic octupole vibrations [51]). In our opinion this explanation is not in contradiction with the concept of stable octupole deformation [see e.g. discussion of the ^{229}Th spectrum in ref. [2])].

The generous support from T. Berggren and the valuable discussions and comments from G. Leander are gratefully acknowledged. A part of the calculations was performed during the stay of one of the authors (W.N.) at the Max-Planck-Institut in Heidelberg. He would like to express his gratitude to the members of the Crystal-Ball group that have shown so much hospitality and assistance.

References

1) G.A. Leander, R.K. Sheline, P. Möller, P. Olanders, I. Ragnarsson and A.J. Sierk, Nucl. Phys. **A388** (1982) 452
2) G.A. Leander and R.K. Sheline, Nucl. Phys. **A413** (1984) 375
3) W. Nazarewicz, P. Olanders, I. Ragnarsson, J. Dudek, G.A. Leander, P. Möller and E. Ruchowska, Nucl. Phys. **A429** (1984) 269
4) W. Nazarewicz, P. Olanders, I. Ragnarsson, J. Dudek and G.A. Leander, Phys. Rev. Lett. **52** (1984) 1272; **53** (1984) 2060
5) M. Gai, J.F. Ennis, M. Ruscev, E.C. Schloemer, B. Shivakumar, S.M. Sterbenz, N. Tsoupas and D.A. Bromley, Phys. Rev. Lett. **51** (1983) 646
6) D. Ward, G.D. Dracoulis, J.R. Leigh, R.J. Charity, D.J. Hinde and J.O. Newton, Nucl. Phys. **A406** (1983) 591
7) W. Bonin, M. Dahlinger, S. Glienke, E. Kankeleit, M. Krämer, D. Habs, B. Schwartz and H. Backe, Z. Phys. **A310** (1983) 249
8) C. Mittag, J. Fernandez-Niello, F. Riess and H. Puchta, Proc. Workshop on electromagnetic properties of high spin states, Rehovot, Israel, January 1984;
C. Mittag, C. Lauterbach, H. Puchta, F. Riess, A. Celler, C. Briancon, A. Lefebvre, J. Fernandez-Niello, J. Żylicz and R. Kulessa, Beschleunigerlaboratorium der Universität und der Technischen Universität Munchen, Jahresbericht 1983, p. 49;
J. Fernandez-Niello, C. Mittag, H. Puchta, F. Riess and D. Selbmann, *ibid.*, p. 51
9) A. Celler, Ch. Briancon, J.S. Dionisio, A. Lefebvre, Ch. Vieu, J. Żylicz, R. Kulessa, C. Mittag, J. Fernandez-Niello, Ch. Lauterbach, H. Puchta and F. Reiss, Nucl. Phys. **A432** (1985) 421;
P.D. Cottle, J.F. Shriner Jr., F. Dellagiacoma, J.F. Ennis, M. Gai, D.A. Bromley, J.W. Olness, E.K. Warburton, L. Hildingsson, M.A. Quader and D.B. Fossan, Phys. Rev. **C30** (1984) 1768
10) W. Bonin, M. Dahlinger, H. Backe, S. Glienke, D. Habs, E. Hanelt, E. Kankeleit and B. Schwartz, Max-Planck-Institut für Kernphysik, Heidelberg, Jahresbericht 1983, p. 96
11) R. Zimmermann, thesis, Universität München, 1980
12) A.L. Goodman, Nucl. Phys. **A230** (1974) 466
13) A. Bohr and B.R. Mottelson, Nuclear structure, vol. 2 (Benjamin, New York, 1975)
14) M. Faber, Phys. Rev. **C24** (1981) 1047
15) M. Faber and M. Ploszajczak, Phys. Scripta **24** (1981) 189
16) S. Frauendorf and V.V. Pashkevich, Phys. Lett. **141B** (1984) 23
17) R. Bengtsson and S. Frauendorf, Nucl. Phys. **A327** (1979) 139

18) W. Kurcewicz, N. Kaffrell, N. Trautmann, A. Plochocki, J. Żylicz, K. Stryczniewicz and I. Yutlandov, Nucl. Phys. **A270** (1976) 175
19) W. Kurcewicz, N. Kaffrell, N. Trautmann, A. Plochocki, J. Żylicz, M. Matul and K. Stryczniewicz, Nucl. Phys. **A289** (1977) 1
20) E. Ruchowska, W. Kurcewicz, N. Kaffrell, T. Björnstad and G. Nyman, Nucl. Phys. **A383** (1982) 1
21) K. Hardt, P. Schuler, C. Gunther, J. Recht, K.P. Blume and H. Wilzek, Nucl. Phys. **A419** (1984) 34
22) Ch. Lautenbach, J. de Boer, Ch. Mittag, F. Rieß, Ch. Schandera, Ch. Briançon, A. Lefebvre, S. Hlavač and R.S. Simon, Phys. Lett. **140B** (1984) 187
23) R.S. Simon, R.P. Devito, H. Emling, R. Kulessa, Ch. Briançon and A. Lefebvre, Phys. Lett. **108B** (1982) 87
24) P. Vogel, Phys. Lett. **60B** (1976) 431
25) H.J. Krappe and U. Wille, Nucl. Phys. **A124** (1969) 641
26) K. Neergård and P. Vogel, Nucl. Phys. **A145** (1970) 33
27) K. Neergård and P. Vogel, Nucl. Phys. **A149** (1970) 217
28) S.G. Rohoziński and W. Greiner, Phys. Lett. **128B** (1983) 1
29) S.G. Rohoziński, M. Gajda and W. Greiner, J. of Phys. **G8** (1982) 787
30) I. Ahmad, R.R. Chasman, J.E. Gindler and A.M. Friedman, Phys. Rev. Lett. **52** (1984) 503
31) A. Bohr and B. Mottelson, Nucl. Phys. **4** (1957) 529; **9** (1958) 687
32) V.M. Strutinsky, J. Nucl. Energy **4** (1957) 523
33) R. Zimmermann, Phys. Lett. **113B** (1982) 199
34) Ch. Briançon and I.N. Mikhailov, Dubna Preprint E4-81-402, Proc. XX Int. Winter Meeting on nuclear physics, Bormio, January 1982, ed. I. Iori, p. 183
35) M. Diebel and U. Mosel, Z. Phys. **A303** (1981) 131
36) J.L. Egido and P. Ring, Nucl. Phys. **A423** (1984) 93
37) J. Dudek, W. Nazarewicz, J. Skalski, Z. Szymański and S. Ćwiok, to be published
38) S.A. Ahmad, W. Klempt, R. Neugart, E.W. Otten, K. Wendt and C. Ekström, Phys. Lett. **133B** (1983) 47
39) C.M. Lederer and V.S. Shirley, ed., Table of isotopes, 7th ed. (Wiley, New York, 1978)
40) I. Ragnarsson, Phys. Lett. **130B** (1983) 353
41) R.K. Sheline and G.A. Leander, Phys. Rev. Lett. **51** (1983) 359
42) R.K. Sheline, D. Decman, K. Nybø, T.F. Thorsteinsen, G. Løvhøiden, E.R. Flynn, J.A. Cizewski, D.K. Burke, G. Sletten, P. Hill, N. Kaffrell, W. Kurcewicz, G. Nyman and G. Leander, Phys. Lett. **133B** (1983) 13
43) R.R. Chasman, Proc. Workshop on semiclassical methods in nuclear physics, Grenoble, March 6–8, 1984, J. de Phys., in press
44) J. Dudek, W. Nazarewicz and Z. Szymański, Phys. Rev. **C26** (1982) 1708
45) J. Dudek, W. Nazarewicz and Z. Szymański, Phys. Scripta **T5** (1983) 171
46) W. Nazarewicz and P. Olanders, to be published
47) S. Frauendorf and F.R. May, Phys. Lett. **125B** (1983) 245
48) G.A. Leander, S. Frauendorf and F.R. May, Proc. Conf. on high angular momentum properties of nuclei, Oak Ridge, 1982, ed. N.R. Johnson (Harwood Academic, New York, 1983), p. 281
49) F. Iachello and A.D. Jackson, Phys. Lett. **108B** (1982) 151
50) H. Daley and F. Iachello, Phys. Lett. **131B** (1983) 281
51) R. Piepenbrink, Phys. Rev. **C27** (1983) 2968